Absolute quantitation of serum antibody reactivity using the Richards growth model for antigen microspot titration

Krisztián Papp, Ágnes Kovács, Anita Orosz, Zoltán Hérincs, Judit Randek, Károly Liliom, Tamás Pfeil, József Prechl

Author information

These authors contributed equally: Krisztián Papp, Ágnes Kovács, Anita Orosz

R&D Laboratory, Diagnosticum Zrt, Budapest, Hungary

Krisztián Papp, Zoltán Hérincs, József Prechl

Department of Applied Analysis and Computational Mathematics, Eötvös Loránd University, Budapest, Hungary

Ágnes Kovács, Tamás Pfeil

Department of Immunology, Eötvös Loránd University, Budapest, Hungary

Anita Orosz

BME, Budapest University of Technology and Economics, Budapest, Hungary

Judit Randek

Department of Biophysics and Radiation Biology, Semmelweis University, Budapest, Hungary

Károly Liliom

Corresponding author: József Prechl, jprechl@diagnosticum.hu

1047 Attila út 126. Budapest, Hungary; T: +36-1-8810161

Current addresses

Anita Orosz : Department of Physiology, Semmelweis University, Budapest, Hungary;

Judit Randek : F. Hoffmann - La Roche Ltd., Basel, Switzerland

Abstract

In spite of its pivotal role in the characterization of humoral immunity, there is no accepted method for the absolute quantitation of antigen specific serum antibodies.

We devised a novel method to quantify polyclonal antibody reactivity, which exploits protein microspot assays and employs a novel analytical approach. Microarrays with a density series of disease specific antigen were treated with different serum dilutions and developed for IgG and IgA binding. By fitting binding data of both dilution series to a product of two generalized logistic functions, we obtained estimates of antibody reactivity of two immunoglobulin classes simultaneously. These estimates are the antigen concentrations required for reaching the inflection point of thermodynamic activity coefficient of antibodies and the limiting activity coefficient of antigen.

By providing universal chemical units, this method may improve standardization of serological testing, the quality control of antibodies and the quantitative mapping of antibody-antigen interaction space.

Keywords:

polyclonal, antibody, quantitative, serology, immunoglobulin, antigen, immune response, chemical potential, activity coefficient, microarray, Richards curve

Introduction

Antibodies are glycoproteins belonging to the immunoglobulin protein superfamily, produced by B cells of the adaptive immune system. Antibodies in an organism are structurally highly heterogeneous owing to the gene recombination-mediated diversity of the adaptive immune response and the clonal nature of B-cell expansions[1,2]. A single given B cell and its progeny of plasmablasts and plasma cells produce antibody molecules with a given target specificity and binding affinity, determined by the fit of the rearranged heavy and light chain variable regions. Millions of B cells carrying different rearranged heavy and light chain variable regions generate a network of diverse antibodies present in an individual [3]. A humoral immune response against a particular antigen involves the evolution of antibody producing plasmablast and plasma cell clones with various isotypes and affinities, these latter properties also being characteristic for the polyclonal response besides target specificity. The affinity of an antibody molecule towards its target antigen is an important characteristic both from the biochemical and immunological point of view. Biochemically, it reflects the strength of interaction between the two binding partners [4]. Immunologically, it is closely correlated with effector functions such as neutralization efficiency and complement activation [5]. The isotype of the antibody molecule is the other key determinant of effector function. Understanding these properties of serum antibodies generated against particular antigenic targets is the goal of serological measurements, which aim at the laboratory diagnosis of infectious, allergic and autoimmune diseases [6–8]. Evidently, medical laboratory diagnostics requires the standardization of serological measurements.

Standardization of the measurement of antibody reactivity has always been a difficult issue [9] and in spite of much effort it has not been fully resolved [10]. Among the analytical issues is the fact that the quantitation of a heterogeneous population of antibodies would require a heterogenous reference material. Currently this is achieved by the utilization of affinity purified polyclonal serum pools or pools of monoclonal antibodies. These reagents, along with the standardization and harmonization of measurement protocols led to current best laboratory practices, which provide results in international units. However, quantitative comparison of different assays with different units is not meaningful, therefore systems level quantitative representation of antibody reactivity is currently impossible.

Determination of antibody affinity has always been considered of key importance for the characterization of humoral immunity. From the immunochemical and biophysical point of view, the techniques employed range from equilibrium dialysis [11], precipitation assays using radiolabeling [11], use of denaturants to disrupt binding forces [12], setting up competition assays

85 [13] and varying Ag density in enzyme-linked immunosorbent-assays (ELISA) [14]. A non-
86 competitive ELISA [15] for the measurement of monoclonal antibody affinity that relies on the
87 determination of Ab binding at different antigen coating densities shares some conceptual basis
88 with our assay, however it requires the use of known concentrations of monoclonal antibodies.
89 Alternatively, equilibrium binding constants can be obtained from kinetics measurements by
90 surface plasmon resonance analysis [16], biolayer interferometry [17], microscale thermophoresis
91 [18] and similar technologies. While these measurements are often regarded as the golden
92 standard of affinity determination, the instrumentation and data-intensive nature of
93 measurement may not be optimal for routine diagnostic use. Additionally, label-free methods
94 are not easily adaptable for the selective measurement of antibody classes, a must for
95 immunodiagnostics.
96 Serum antibody titration is a simple and widely used way of estimating antibody reactivity,
97 wherein the sample is serially diluted and the highest dilution that gives a signal reliably
98 discernible from the background, or the dilution resulting in half signal, are regarded as the
99 titer for endpoint and midpoint titration, respectively. Such titers may provide fast and cost-
100 effective semi-quantitative results but are not suitable for real quantitation of serum antibodies
101 because we are changing an unknown variable when we decrease antibody concentration by
102 serum dilution.
103 The unique properties of microspot immunoassays were described by Ekins [19], who propagated
104 their use for capture immunoassays [20]. The general idea is that owing to the negligible amount
105 of molecules present in the microspot probe compared to the amount of analyte in the tested
106 solution, these assays are mass independent [20]: interactions are governed by concentration and
107 affinity only. When affinity is constant and homogenous, as in a capture immunoassay utilizing
108 monoclonal antibody, the density of analyte bound to the surface is determined solely by its
109 concentration. Here we propose that mass independence of microspot immunoassays in fact
110 requires an analytical approach that is different from conventional calculations based on the
111 law of mass action [15,21], which applies to reactions in solutions. We suggest the use of concepts
112 and terminology of physical chemistry, which are readily applicable to reactions at a solid-
113 liquid interface [22,23].
114 In this paper we present a microspot-based approach that allows the estimation of apparent
115 chemical potential of distinct antibody isotypes in human serum without any prior purification
116 steps. The measurement relies on the simultaneous titration of antigen surface density and
117 serum dilution and on an improved mathematical model of fitting. Most importantly, by
118 changing a known variable of the system, antigen concentration, the technology allows the

absolute quantification of antigen specific reactivity of polyclonal serum antibodies, allowing quantitative comparison of different samples, isotypes or antigens.

Results

Experimental setup and properties of the measurement system

The experimental system we use is characteristic of protein microarray technology with some key differences to traditional indirect ELISA. The solid surface used as antigen adsorbent has higher binding capacity than conventional polystyrene. This results in a dose dependent adsorptive binding over a wider concentration range. Therefore, the concentration of antigen in the solution used for bio-printing (spotting of antigen) is expected to show linear relationship with the surface density of the antigen on the microarray over a correspondingly wider range. Antibodies that bind to the spotted antigens are detected by fluorescently labelled secondary antibodies. Owing to the properties of fluorescent measurement, bound antibodies can be detected over a wide range as well. To allow for the analysis and visualization of signals spreading over several orders of magnitude, the logarithm of both antigen concentrations and fluorescent signal intensities is used.

To establish a distribution of immune complex concentrations as a function of antigen density we employed two different, complementary strategies (Fig. 1). First, increasing concentrations of antigen [Ag] were printed on a solid surface as microspots. Owing to the negligible amount of antigen in a microspot compared to the amount of antibody in the reaction solution, these measurement conditions are called mass-independent or ambient analyte immunoassay [19,20]. Antigen microspots therefore probe antibody reactivity in the sample without significantly altering composition of the sample. Second, dilutions of the serum samples of interest were prepared to vary the concentration of antibody-antigen complexes [AbAg] in the measurement range and to examine the relationship between antibody concentration [Ab] and [AbAg]. Even though the absolute free antibody concentration [Ab] in the tested serum is not known, the relative concentrations of the dilution series can be used to follow [Ab] effects by mathematical curve fitting. Dilutions of serum samples were applied to the series of antigen density microspots and incubated to bring the system in equilibrium.

Figure 1. Simultaneous titration of antigen density and serum antibody

151 The resulting measurement system examines the effect of changes in relative [Ab] and [Ag] on
152 the extent of Ab binding. The obtained experimental data are fitted with a growth function to
153 derive values of the parameters that characterize antibody reactivity in the sample (Fig. 1).
154
155 *Curve fitting*
156 The formation of AbAg complexes and the extent of antibody binding under equilibrium in our
157 assay can be interpreted as the indicator of Ab thermodynamic activity in the microspots. The
158 equilibrium concentration of AbAg complexes is a logistic function of ln[Ag], and the
159 logarithm of the fluorescent intensity is a linear function of ln[AbAg], therefore the growth of
160 fluorescent intensity can be described by the generalized logistic function [24,25] or Richards
161 function R(x) of x=ln[Ag], an extended form of the function most frequently used for
162 immunoassays. We use the following parametrization
163 $$R(x) = A * (1 + (d-1)e^{-k*(x-x_i)})^{\frac{1}{1-d}} \quad (1$$
164 where A is Ab capacity, [Ab]; k is rate of exponential growth; d determines asymmetry, the
165 relative value of R at fastest growth; x_i is the point of fastest growth or inflection point.
166 The capacity of the system is determined by the availability of antibody, [Ab]. While the exact
167 value is unknown, relative values corresponding to steps in dilution series can be used in the
168 fitting procedure. In our assay exponential growth of [AbAg] is allowed by the provision of
169 exponentially increasing [Ag] in a series of microspots. We assume that antigen titration results
170 in a binding curve following a generalized logistic curve with the rate of exponential growth
171 k=1, which corresponds to $[Ag]=e^{1*\ln[Ag]}$. Shape parameter d of the generalized logistic function
172 allows for asymmetry in the binding curve. In our assay d is an index, which characterizes the
173 Ab composition of serum. Location of the fastest growth x_i with respect to ln[Ag] provides a
174 general measure of antibody affinity.
175 Affinities and concentrations of serum antibodies are distributed over a very wide range,
176 equilibrium dissociation constants from 10^{-5} to 10^{-11} and molar concentrations from pM to nM,
177 respectively. In order to better assess interactions over this range and to weigh curve fitting
178 against signal intensity-dependent variation, we use logarithmically transformed signals of
179 binding. Thus, fitting the Richards curve to our measurements therefore requires the
180 logarithmic form of the above equation
181 $$\ln R(x) = \ln(A) + \frac{1}{1-d} * \ln\left(1 + (d-1) * e^{-k*(x-x_i)}\right) \quad (2$$

182 By using the logarithm we transform thermodynamic activity to chemical potential of the Ab,
183 as determined by its standard molar Gibbs free energy, concentration and activity coefficient

184 $$\mu_{Ab} = \mu^{\circ} + RTln(a_{Ab}) = \mu^{\circ} + RTln(c_{Ab} * \gamma_{Ab}) = \mu^{\circ} + RTln(c_{Ab}) + RTln(\gamma_{Ab}) \quad (3$$

185 where μ is chemical potential; μ° is standard chemical potential or molar Gibbs free energy;
186 a is relative thermodynamic activity; γ is activity coefficient; and c is molar concentration.
187 Since the standard term serves as a reference point, we can still obtain relative potentials after
188 its removal. Then we can interpret ln(A) of the lnR(x) function as the mole fraction term of
189 chemical potential and the remaining part of the function describes the activity coefficient as a
190 function of [Ag] (for details see **Supplementary text 1**).
191 To demonstrate the dependence of ln(A) from the serum dilution we extended the formula of
192 lnR(x) to obtain the combined fitting of serum dilutions and antigen dilutions:

193 $$\mathrm{lnR}_2(x,z) = \ln(C) - m * \ln(B+z) + \frac{1}{1-d} * \ln\left(1 + (d-1) * e^{-(x-x_i)}\right) \quad (4$$

194 where z is serum dilution, and m, B, C are auxiliary parameters of the logarithm of another
195 generalized logistic function(Tjørve and Tjørve 2010) of -ln(z) that replaced ln(A) and has a
196 parametrization different from formula (2.
197 Reliable curve fitting depends on the number and location of x=ln[Ag] measurement points on
198 the curve and requires the value of x_i to be in the measurement range.
199
200 *Characterization of anti-deamidated gliadin peptide serum antibodies*
201 As an exemplary antigen for the proof of our measurement principle we choose a deamidated
202 peptide sequence known to be the target of antibodies in celiac disease. Such an antigenic
203 peptide is a well-defined molecular target of both IgA and IgG antibodies in celiac patients and
204 is used in laboratory diagnostics. We used peptide concentrations corresponding to the range
205 of K_D values expected to occur in serum and peptide dilutions that well extended beyond that
206 range. Serum samples were diluted to span about two orders of magnitude and correspond to
207 dilutions conventionally used in serological diagnostics. Binding data were fitted using the
208 $\mathrm{lnR}_2(x)$ function of equation (4 introduced above and generated curves were overlain on the
209 binding data (Fig. 2)
210
211 *Figure 2. Fitting in two dimensions*
212

213 Using the values of parameters from the fitted binding curves of experimental data, we can
214 generate binding curves normalized to Ab concentrations, which are curves of thermodynamic
215 activity coefficients γ_{Ab}, as illustrated in Figure 3.
216
217 *Figure 3. Comparative characterization of serum antibody binding*
218
219 These curves are independent of antibody concentrations and fluorescent intensity and are
220 therefore comparable for different classes of Ab in a given sample, for different samples and
221 any combination thereof. Parameter x_i and γ_{Ab} are sufficient to quantitatively characterize the
222 distribution of Ab thermodynamic activity in the tested serum sample as long as the Richards
223 curve models binding events.
224 To confirm that conventional titration cannot provide exact results we calculated titers from
225 the binding data obtained from the microspot experiments. The classical approach of serum
226 titration was heavily dependent on the antigen density, as observed by others [13,26,27]. We
227 calculated end-point titers and mid-point titers of the same measurements by logistic fitting of
228 binding curves to distinct antigen densities, and obtained different titers for different antigen
229 densities (Fig. 4). This antigen density dependence is not only avoided but is instead exploited
230 in our approach of fitting curves to antigen density.
231
232 *Figure 4. Conventional titration of serum*
233
234 We also confirmed the applicability of our method to other antigens using a microarray printed
235 with dilution series of citrullinated peptides known to be targets of autoantibodies of
236 rheumatoid arthritis patients (**Supplementary Fig. S1**).
237
238 *Measurement of reference monoclonal antibody properties*
239 Current serological assays use standardized antibody preparations as reference material for
240 quality control and calibration [10]. These preparations are monoclonal antibodies alone or in
241 combinations of monoclonal antibodies, or pooled raw or isolated serum antibodies from
242 positive samples. Because of the individual variance of affinity distribution of serum antibodies
243 these approaches have the major drawback of assuming identical affinity distribution of
244 reference and test samples. Titration by antigen density avoids this pitfall since it does not a
245 priori assume but it rather identifies distribution of samples and reference standards. The
246 incorporation of a reference antibody is also suitable to control antigen density variation. A

247 critical point of antigen density titration is the precise deposition of Ag on the microarray
248 surface, so that the real density of antigen corresponds to the nominal antigen concentration
249 used for printing. The precision can be estimated by measuring and characterizing a reference
250 antibody. We successfully used the monoclonal antibody 14D15 specific for an epitope in our
251 deamidated gliadin peptide sequence to characterize their interaction (Fig. 5).
252
253 *Figure 5. Characterization of a monoclonal Ab*
254
255 **Discussion**
256 The concentrations of serum antibodies and of targets of these antibodies, along with the range
257 of the strength of these interactions span several orders of magnitude. To obtain a systems level
258 structured map of these interactions we need technologies that provide quantitative results of
259 molecular interaction measurements over this wide range, from low picomolar to micromolar
260 concentrations. Here we present results, which together with earlier observations [28,29] provide
261 evidence and theoretical support for protein microspot-based fluorescent detection as a method
262 of choice.
263 The difficulty of rendering the measurement of polyclonal antibody responses quantitative lies
264 partly in the reproducible generation of rigorously characterized antigen, partly in the
265 mathematical description of heterogeneity of polyclonal antibody response. The generation of
266 synthetic epitopes for serological assays, along with functional characterization using reference
267 affinity reagents may solve the first issue [10,30]. Our approach may provide a solution for the
268 second one: establishing standardized assays that generate quantitative data with SI units of
269 measurement. The key for generating a quantitative description of polyclonal serum antibody
270 reactivity is the ability to dissect antibody concentration and affinity, the two parameters that
271 determine antigen saturation. This is basically achieved by titrating both concentration and
272 affinity: in addition to the conventional serum dilution series, a series of antigen dilutions is
273 used concomitantly. By diluting serum antibody, a series of antibody concentrations is
274 examined, while by additionally using microspots of antigen dilution series, affinity
275 distribution is assessed simultaneously. Microspots allow a mass-independent interrogation of
276 interactions on the chip surface, whereby the measurement becomes independent of the relative
277 total masses of Ag and Ab in the reaction volume. Complex formation is determined only by
278 concentration and affinity, which two measures can be deconvolved by two-dimensional
279 titration. By gradually increasing the Ag density of the surface, an Ab with a given affinity will
280 engage in lower affinity interactions as well. This results in the measurement of a range of

affinities from the highest (detected on low density Ag spots) to more degenerate lower affinity interactions.

There have been several attempts to characterize the affinity of antibodies associated with autoimmunity [31–34], infectious disease [35,36], vaccination [37] and allergy [14,38–41]. The strength of binding of serum antibodies is determined by the distribution of clones with different affinities specific for the tested epitope. While the importance of antibody affinity in conferring pathogenicity or protectivity is widely acknowledged, affinity determination is not generally considered as part of diagnostic serology. The possible reason is that affinity measurement is technologically challenging and is not standardized, as outlined above. Affinity dependence of traditional immunoassays (e.g., RIA, ELISA, Farr assay, hemagglutination, complement-mediated haemolysis, precipitation) [42] practically excludes low affinity interactions from measurement and may skew affinity determinations when such assays are used. Such a progressive decrease of sensitivity to low affinity antibodies should lead to estimations of antibody affinity distribution with a higher mean affinity. The method we propose here presumes the existence of low affinity antibodies and measures them by using Ag at very high densities as well.

Microspot immunoassays were introduced for the measurement of analyte concentration, taking advantage of the very low amount of capture antibody required by the technology. If in the complete volume of measurement, the concentration of antibody on the solid support is less than 1% of the K_D of interaction, then the concentration of the analyte does not change significantly (<1%) during the measurement. The signal from a detection antibody is therefore correlated only with analyte concentration when other variables are kept constant, which conditions are characteristic of ambient analyte immunoassay [19]. The analyte in our assay is serum antibody and the K_D of interactions are heterogeneous. Nevertheless, the amount of antigen and therefore its concentration in the total measurement volume is still negligible. Our method takes further advantage of microspots by varying the surface density of antigen for antibody capture. Since the relative concentrations of antibodies with different affinities are not changed by serum dilution, the affinity profile of antibodies that make contact with antigen on the solid support does not change either. The activity coefficient of this population of antibodies will depend solely on the density of antigen [Ag] relative to the average affinity of interactions. By varying [Ag] we obtain a distribution curve of chemical potentials suitable for estimating values of the parameters of fitted function.

The interpretation of Richards curve parameters provides insight into several aspects of serum antibody reactivity. Parameter A is related to the molar concentration of functional antibody

315 binding sites, called paratopes, belonging to the measured immunoglobulin class. Because the
316 measurement of distribution of affinity reaches into the low affinity range, the estimated
317 concentrations are approximations of total serum antibody concentrations. We expect this value
318 to be dependent and correlated with serum antibody concentrations and therefore to have less
319 diagnostic value. Thus, it is presumably not necessary to adjust for antibody valency and
320 convert binding site concentrations into isotype concentrations. Antibody responses that exploit
321 the increase of antibody concentrations without major increase in affinity, like the thymus-
322 independent response, are therefore expected to appear as a change in this parameter. A
323 technical advantage of rendering the binding parameters independent of total serum antibody
324 concentrations is that we also exclude absolute fluorescence intensity values from the analysis,
325 thus removing a factor of interlaboratory variance.
326 The central point or inflection point x_i is related to the apparent chemical potential of serum
327 antibodies. We propose to use the short name "$\ln K_D$" for the natural logarithm of molar
328 concentration of antigen required to reach maximal relative growth of antibody activity
329 coefficient γ_{Ab} (inflection point of sigmoid curve in log-lin scale). While the unit of chemical
330 potential is that of energy (Joule/mole) here we would retain the unitless number derived from
331 antigen concentration titration.
332 The Richards curve uses parameter d to introduce asymmetry on the two sides of the inflection
333 point. At d=2 the curve is symmetric and it is a logistic curve. At d→1 the curve approaches
334 the Gompertz growth curve and becomes asymmetric as the inflection point shifts from y_i=A/2
335 to y_i=A/e.
336 The slope of the $\ln R_2(x)$ function s=k/(d-1) at minus infinity, in the case k=1, meanwhile
337 increases from s=1 to ∞. This slope characterizes interactions as antigen is diluted out to
338 infinity. Infinite dilution is a special thermodynamic state when antigen molecules are in
339 contact with antibody molecules only [43]. In this state binding is determined only by interactions
340 between Ag and Ab, without the interference of homotypic interactions. This ideal state is
341 characterized by the limiting activity coefficient γ_i^{∞}. Using our parametrization d-1 changed
342 between 0 and 1. We propose that d-1 is the limiting activity coefficient of Ag, γ_{Ag}^{∞}. It
343 characterizes the composition of Ab mixture with 0 representing no interacting Abs and 1
344 representing 100% presence of binding Abs at infinite Ag dilution. We expect that parameter
345 d can be used to characterize disease activity when antibody diversity and affinity is related to
346 disease pathogenesis, with lower d implying immunological activity, and higher d indicating
347 approach of equilibrium concentrations and stability of the immune response.

348 A potential disadvantage of the proposed method is that it is technologically challenging,
349 compared to established automated assays. A critical point is the generation of antigen spots
350 with real densities as close to nominal densities as possible. This requires the introduction of
351 extra quality control steps into the production. The fitting procedure requires a minimal number
352 of data points around the estimated inflection point, therefore weakly reactive samples cannot
353 be quantitated. These disadvantages position our assay as a fine analysis method, suitable not
354 for the screening and identification of presence of specific antibodies but rather for the detailed
355 characterization of pre-screened sera.
356 A key conceptual novelty in our assay is that instead of assessing the concentration of a
357 heterogeneous antibody population we assess distribution of apparent chemical potential.
358 Current immunoassays focus on establishing conditions that are ideal for estimation of the
359 concentration of antibodies against a particular target antigen. For solid phase assays this
360 involves the optimization of coating antigen density, where actually an antigen density suitable
361 for identifying the shift of average K_D in a diagnostically relevant region of affinity is
362 identified. By using microspots with antigen densities spanning the whole range of relevant
363 concentrations, a single measurement can provide a distribution of apparent Ab chemical
364 potentials.
365 The procedure we describe here assumes that equilibrium is reached when microspots are
366 incubated in serum. In order to confirm that measurement conditions are appropriate and to
367 allow reproducibility and interassay comparisons, antibody standards can be introduced into
368 the assay. Pooled positive and borderline serum samples could be used in our assay just as in
369 any other immunoassay for specific antibody measurement. Additionally, monoclonal antibody
370 preparations are also suitable as internal reference, since calculations of sample Ab affinity
371 would not be based on the binding of reference antibody, but these would rather serve as
372 controls for validation and perhaps for adjusting calculations.
373 The introduction of such quantitative assays could not only improve diagnostic accuracy of
374 immunoassays but would also pave the way to our quantitative understanding of the adaptive
375 immune system. The generalized quantitative model of antibody homeostasis [3] provides a
376 conceptual framework for the experimental mapping of the "antibodyome" [44–46], a goal that
377 could be achieved by the strategic mapping of antigen structural space. The integration of
378 quantitative binding information into a network and the mapping of the interaction network [45]
379 to the sequence space generated by next generation sequencing [47] is expected to bring about
380 unprecedented systemic understanding of adaptive immunity in particular and protein
381 evolution in general.

382

383 **Materials and methods**

384 *Microarray production and measurements*

385 Experiments were carried out on hydrogel coated glass slides (Nexterion Slide H) by using a
386 BioOdyssey Calligrapher MiniArrayer. Different peptide dilutions, as indicated in the text,
387 were spotted in quintuplicates of ½ serial dilution in 7 steps starting from 200 µM. Slides were
388 dried for 1h at 37°C then soaked in 0.1 M Tris buffer (pH=8) for 1h at 37°C in order to block
389 reactive residues on the surface. Once prepared, slides were kept in sealed non-transparent bags
390 at 4 °C. The fusion peptide GLN1-2F was based on the deamidated gliadin sequence motifs
391 LQPFPQPELPYPQPQ and PLQPEQPFP.

392 Previously characterized, frozen serum samples collected for studies with contract numbers:
393 24933-6/2018/EKU and 24973-1/2012/EKU (658/PI/2012.) were used for the experiments.
394 Those studies were aimed at developing serological assays for gluten sensitivity and
395 autoimmune diseases, respectively, and all procedures were in accordance with the ethical
396 standards of the responsible committee on human experimentation and with the Helsinki
397 declaration of 1975, as revised in 2008.

398

399 *Sample handling and signal detection*

400 The basic protocol was the following: dried arrays were rehydrated in 110 µl PBS (3×5 min)
401 before using, then sub-arrays were incubated in 70 µl diluted sample at 37 °C for 1 h. Sample
402 dilution was carried out in PBS-BSA-Tween (PBS, 2% BSA, 0.05% Tween 20). Serum treated
403 slides were washed in 0.05% Tween-PBS, then incubated at room temperature for 30 minutes
404 with fluorescently labelled antibodies that were diluted in the blocking buffer (0.05% Tween
405 20, 2% BSA, PBS). Detecting antibodies were the following: Fc γ fragment specific DyLight
406 649-conjugated AffinityPure F(ab')2 fragment goat anti-human IgG; DyLight 549-conjugated
407 AffinityPure F(ab')2 fragment goat anti human-IgA. Chips were washed again and following
408 drying, slides were scanned using laser microarray scanner.

409

410 *Measurements with 14D5 monoclonal antibody*

411 The previously described basic protocol was altered for the assays with monoclonal antibody
412 against deamidated gliadin (14D5). First, slides were rehydrated in PBS (3×5 min) then blocked
413 in blocking buffer (0.05% Tween 20, 2% BSA, PBS) for 30 minutes at 37°C. A dilution series
414 was prepared from the monoclonal antibody starting from 200 µg/ml by ½ in 10 steps.
415 Detection was carried out by goat anti-mouse IgG2a-Alexa488.

416

417 *Analysis of the microarray data*

418 Images of the slides were analyzed with GenePix Pro 6.0 software after visual inspection. Spots
419 were recognized by the program, then gpr files containing the spot coordinates for individual
420 spots were created. Then R (version 3.5.2), a statistical programming environment, was used
421 to re-analyse 16-bit tiff images by using these coordinates in order to align the spots. Relative
422 fluorescence intensity (RFI) medians were calculated for each spot using 80% of the diameter
423 of the circle shapes that were previously adjusted on the features by the software. In the next
424 step, means of the 5 parallel spots were taken and values of the least concentration antigen
425 spots (considered as background) were subtracted of all RFI values, thus providing the final
426 signal intensities.

427

428 *Fitting of binding curves*

429 In the indirect assay, we take into consideration that a bound antibody inhibits nearby free
430 antigens from forming complexes with other antibodies [48,49]. This inhibition makes the
431 concentration of immune complexes a logistic function of the logarithm of the total antigen
432 concentration:

433 $$[AbAg] = [Ab] * [Ag]/(K_D + [Ab] + D * [Ab] * [Ag]) \quad (6$$

434 where D is positive constant.

435 It is the nature of our measurement system that the logarithm fluorescent intensity is a linear
436 function of the logarithm concentration of AbAg complexes. By using these, we obtain that the
437 logarithm of fluorescent intensity is a Richards function of the logarithm of total antigen
438 concentration

439 $$R(x) = A * (1 + (d - 1) * e^{-k(x - x_i)})^{\frac{1}{1-d}} \quad (7$$

440 with k = 1, where A is the total antibody concentration [Ab] (limit of function R(x) at infinity),
441 x_i is the inflection point, d is the asymmetry parameter.

442 The upper limit of the fluorescent intensity A depends on the serum dilution. Formula (6) also
443 implies that the concentration of immune complexes is a logistic function of the logarithm of
444 the total antibody concentration ln[Ab] with growth rate 1, i.e. a logistic function of −ln(z) with
445 growth rate 1, where z is the serum dilution factor. Due to the linear dependence of the
446 logarithm fluorescent intensity on the logarithm printed Ag concentration, the upper limit of
447 the logarithm fluorescent intensity is a Richards function of the negative logarithm serum
448 dilution z with growth rate 1.

Therefore, the fluorescent signal intensity against the logarithm total antigen concentration x, and the negative logarithm of serum dilution, -ln(z), is the product of two generalized logistic functions of form

$$R_2(x,z) = C * (B+z)^{-m} * (1+(d-1) * e^{-(x-x_i)})^{\frac{1}{1-d}} \quad (8$$

The logarithm transformation converts the proportional variance pattern to a constant variance pattern and thus the conversion makes the transformed data more suitable for fitting the model. The above multiplicative relationship now changes to an additive one in the form of

$$lnR_2(x,z) = \ln(C) - m * \ln(B+z) + \frac{1}{1-d} * \ln\,(1+(d-1) * e^{-(x-x_i)}) \quad (9$$

This generalized logistic model on the log-log scale was fit to the data, and parameter estimates and 95% confidence intervals were obtained for each serum and both isotypes. All analyses were carried out using the R software (version 3.5.2).

Nonlinear least squares estimates for the model parameters were calculated using the Gauss-Newton algorithm of the nls function from the statistical software package R (version 3.5.2). The 95% confidence intervals generated for the model parameters were based on the profile likelihood technique.

465 Bibliography

466 1. Imkeller, K. & Wardemann, H. Assessing human B cell repertoire diversity and
467 convergence. *Immunol. Rev.* **284**, 51–66 (2018).

468 2. Briney, B., Inderbitzin, A., Joyce, C. & Burton, D. R. Commonality despite exceptional
469 diversity in the baseline human antibody repertoire. *Nature* **566**, 393–397 (2019).

470 3. Prechl, J. A generalized quantitative antibody homeostasis model: antigen saturation,
471 natural antibodies and a quantitative antibody network. *Clin. Transl. Immunology* **6**,
472 e131 (2017).

473 4. Marillet, S., Lefranc, M.-P., Boudinot, P. & Cazals, F. Novel Structural Parameters of
474 Ig-Ag Complexes Yield a Quantitative Description of Interaction Specificity and
475 Binding Affinity. *Front. Immunol.* **8**, 34 (2017).

476 5. Prechl, J. A generalized quantitative antibody homeostasis model: maintenance of
477 global antibody equilibrium by effector functions. *Clin. Transl. Immunology* **6**, e161
478 (2017).

479 6. Bacarese-Hamilton, T., Bistoni, F. & Crisanti, A. Protein microarrays: from
480 serodiagnosis to whole proteome scale analysis of the immune response against
481 pathogenic microorganisms. *BioTechniques* **Suppl**, 24–29 (2002).

482 7. Meyer, P. W. A., Ally, M. M. T. M. & Anderson, R. Reliable and cost-effective
483 serodiagnosis of rheumatoid arthritis. *Rheumatol. Int.* **36**, 751–758 (2016).

484 8. Chokshi, N. Y. & Sicherer, S. H. Interpreting IgE sensitization tests in food allergy.
485 *Expert Rev. Clin. Immunol.* **12**, 389–403 (2016).

486 9. Bozsóky, S. The problem of standardization in rheumatoid arthritis serology. *Arthritis*
487 *& Rheumatism* **6**, 641–649 (1963).

488 10. Meroni, P. L. *et al.* Standardization of autoantibody testing: a paradigm for serology in
489 rheumatic diseases. *Nat. Rev. Rheumatol.* **10**, 35–43 (2014).

490 11. Stanley, C., Lew, A. M. & Steward, M. W. The measurement of antibody affinity: a
491 comparison of five techniques utilizing a panel of monoclonal anti-DNP antibodies and
492 the effect of high affinity antibody on the measurement of low affinity antibody. *J.*
493 *Immunol. Methods* **64**, 119–132 (1983).

494 12. Macdonald, R. A., Hosking, C. S. & Jones, C. L. The measurement of relative
495 antibody affinity by ELISA using thiocyanate elution. *J. Immunol. Methods* **106**, 191–
496 194 (1988).

497 13. Bruderer, U., Deusinger, M., Schürch, U. & Lang, A. B. Analyses of affinity
498 distributions within polyclonal populations of antigen-specific antibodies. Evaluation of
499 their accuracy in population detection using monoclonal antibodies. *J. Immunol.*
500 *Methods* **151**, 157–164 (1992).

501 14. Nieto, A., Gaya, A., Jansa, M., Moreno, C. & Vives, J. Direct measurement of
502 antibody affinity distribution by hapten-inhibition enzyme immunoassay. *Mol. Immunol.*
503 **21**, 537–543 (1984).

504 15. Beatty, J. D., Beatty, B. G. & Vlahos, W. G. Measurement of monoclonal antibody
505 affinity by non-competitive enzyme immunoassay. *J. Immunol. Methods* **100**, 173–179
506 (1987).

507 16. Sem, D. S., McNeeley, P. A. & Linnik, M. D. Antibody affinities and relative titers in
508 polyclonal populations: surface plasmon resonance analysis of anti-DNA antibodies.
509 *Arch. Biochem. Biophys.* **372**, 62–68 (1999).

510 17. Abdiche, Y., Malashock, D., Pinkerton, A. & Pons, J. Determining kinetics and
511 affinities of protein interactions using a parallel real-time label-free biosensor, the
512 Octet. *Anal. Biochem.* **377**, 209–217 (2008).

513 18. Jerabek-Willemsen, M., Wienken, C. J., Braun, D., Baaske, P. & Duhr, S. Molecular
514 interaction studies using microscale thermophoresis. *Assay Drug Dev. Technol.* **9**,
515 342–353 (2011).

516 19. Ekins, R., Chu, F. & Biggart, E. Multispot, multianalyte, immunoassay. *Ann Biol Clin*
517 *(Paris)* **48**, 655–666 (1990).

518 20. Saviranta, P. *et al.* Evaluating sandwich immunoassays in microarray format in terms
519 of the ambient analyte regime. *Clin. Chem.* **50**, 1907–1920 (2004).

520 21. Larsson, A. Assessment of polyclonal antibody binding of ligand by Sips' equation or
521 by the exact polyclonal equation. Comparison of models. *Mol. Immunol.* **25**, 1239–
522 1249 (1988).

523 22. Kallay, N., Preočanin, T., Kovačević, D., Lützenkirchen, J. & Villalobos, M.
524 Thermodynamics of the reactions at solid/liquid interfaces. *Croat. Chem. Acta* 1–10
525 (2011) doi:10.5562/cca1864.

526 23. Moradi, O. Thermodynamics of Interfaces. in *Thermodynamics - Interaction Studies -*
527 *Solids, Liquids and Gases* (ed. Moreno Pirajn, J. C.) (InTech, 2011).
528 doi:10.5772/20083.

529 24. Gottschalk, P. G. & Dunn, J. R. The five-parameter logistic: a characterization and
530 comparison with the four-parameter logistic. *Anal. Biochem.* **343**, 54–65 (2005).

531 25. Tsoularis, A. & Wallace, J. Analysis of logistic growth models. *Math. Biosci.* **179**, 21–
532 55 (2002).

533 26. Hadzhieva, M. *et al.* Impact of antigen density on the binding mechanism of igg
534 antibodies. *Sci. Rep.* **7**, 3767 (2017).

535 27. Lew, A. M. The effect of epitope density and antibody affinity on the ELISA as
536 analysed by monoclonal antibodies. *J. Immunol. Methods* **72**, 171–176 (1984).

537 28. Kusnezow, W. *et al.* Optimal design of microarray immunoassays to compensate for
538 kinetic limitations: theory and experiment. *Mol. Cell. Proteomics* **5**, 1681–1696 (2006).

539 29. Engelmann, B. W. *et al.* The development and application of a quantitative peptide
540 microarray based approach to protein interaction domain specificity space. *Mol. Cell.*
541 *Proteomics* **13**, 3647–3662 (2014).

542 30. Rizwan, M. *et al.* Serology in the Digital Age: Using Long Synthetic Peptides Created
543 from Nucleic Acid Sequences as Antigens in Microarrays. *Microarrays (Basel)* **5**,
544 (2016).

545 31. Achenbach, P. *et al.* Combined testing of antibody titer and affinity improves insulin
546 autoantibody measurement: Diabetes Antibody Standardization Program. *Clin.*
547 *Immunol.* **122**, 85–90 (2007).

548 32. Szarka, E. *et al.* Affinity Purification and Comparative Biosensor Analysis of Citrulline-
549 Peptide-Specific Antibodies in Rheumatoid Arthritis. *Int. J. Mol. Sci.* **19**, (2018).

550 33. Real-Fernández, F. *et al.* Surface Plasmon Resonance Method to Evaluate Anti-
551 citrullinated Protein/Peptide Antibody Affinity to Citrullinated Peptides. *Methods Mol.*
552 *Biol.* **1348**, 267–274 (2015).

553 34. Sakakibara, S. *et al.* Clonal evolution and antigen recognition of anti-nuclear
554 antibodies in acute systemic lupus erythematosus. *Sci. Rep.* **7**, 16428 (2017).

555 35. Poulsen, T. R., Jensen, A., Haurum, J. S. & Andersen, P. S. Limits for antibody
556 affinity maturation and repertoire diversification in hypervaccinated humans. *J.*
557 *Immunol.* **187**, 4229–4235 (2011).

558 36. Reddy, S. B. *et al.* Differences in affinity of monoclonal and naturally acquired
559 polyclonal antibodies against Plasmodium falciparum merozoite antigens. *BMC*
560 *Microbiol.* **15**, 133 (2015).

561 37. Pratesi, F. *et al.* BNT162b2 mRNA SARS-CoV-2 Vaccine Elicits High Avidity and
562 Neutralizing Antibodies in Healthcare Workers. *Vaccines (Basel)* **9**, (2021).

563 38. Xiong, H., Dolpady, J., Wabl, M., Curotto de Lafaille, M. A. & Lafaille, J. J. Sequential
564 class switching is required for the generation of high affinity IgE antibodies. *J. Exp.*
565 *Med.* **209**, 353–364 (2012).

566 39. Mita, H., Yasueda, H. & Akiyama, K. Affinity of IgE antibody to antigen influences
567 allergen-induced histamine release. *Clin. Exp. Allergy* **30**, 1583–1589 (2000).

568 40. Wang, J. *et al.* Correlation of IgE/IgG4 milk epitopes and affinity of milk-specific IgE
569 antibodies with different phenotypes of clinical milk allergy. *J. Allergy Clin. Immunol.*
570 **125**, 695–702, 702.e1 (2010).

571 41. Pierson, L., Allauzen, S., Blumenthal, M. & Rosenberg, A. An automated method for
572 determination of antibody affinity distribution functions with nanogram quantities. *J.*
573 *Immunol. Methods* **211**, 97–109 (1998).

574 42. Péterfy, F., Kuusela, P. & Mäkelä, O. Affinity requirements for antibody assays
575 mapped by monoclonal antibodies. *J. Immunol.* **130**, 1809–1813 (1983).

576 43. Alessi, P., Fermeglia, M. & Kikic, I. Significance of dilute regions. *Fluid Phase Equilib*
577 **70**, 239–250 (1991).

578 44. Dimitrov, D. S. Therapeutic antibodies, vaccines and antibodyomes. *MAbs* **2**, 347–
579 356 (2010).

580 45. Prechl, J. Network organization of antibody interactions in sequence and structure
581 space: the RADARS model. *Antibodies (Basel)* **9**, (2020).

582 46. Prechl, J. Why current quantitative serology is not quantitative and how systems
583 immunology could provide solutions. *Biologia Futura* (2021) doi:10.1007/s42977-020-
584 00061-1.

47. Prechl, J. Quantitative network organization of interactions emerging from the evolution of sequence and structure space of antibodies: the RADARS model. *BioRxiv* (2018) doi:10.1101/438804.

48. De Michele, C., De Los Rios, P., Foffi, G. & Piazza, F. Simulation and Theory of Antibody Binding to Crowded Antigen-Covered Surfaces. *PLoS Comput. Biol.* **12**, e1004752 (2016).

49. Edwards, D. A. Steric hindrance effects on surface reactions: applications to BIAcore. *J. Math. Biol.* **55**, 517–539 (2007).

Acknowledgments

We thank participants of the GAPAID consortium, especially László Czirják, for providing serum samples for the study and Paolo Rovero for providing VCP2 peptide.

Author contributions

Á.K. analyzed data, developed model, wrote fitting program

J.P. conceptualized of strategy, designed experiments, wrote manuscript, created figures, supervised study

J.R. carried out measurements

K.L. designed experiments

K.P. designed experiments, analyzed data, contributed to figures

O.A. carried out measurement, analyzed data, wrote manuscript

T.P. conceptualized and developed model

Z.H. produced microarrays, carried out measurements

Conflict of interest

K.P., Z.H. and J.P. are employed by Diagnosticum Zrt, a company that provides custom microarray services. A provisional patent application related to this work has been filed by Diagnosticum zrt.

Funding

JP was partially supported by VEKOP-2.1.1-15-2016-00098 grant, part of Széchenyi 2020 project, to Diagnosticum. This work of TP was completed in the ELTE Institutional Excellence Program (TKP2020-IKA-05) financed by the Hungarian Ministry of Human Capacities.

623 **Figure legends**

624

625 **Figure 1**. Simultaneous titration of antigen density and serum antibody

626 Steps of the technology, starting with microarray fabrication and measurement, through image
627 analysis to curve fitting and visualization of results are shown. Serum dilution is indicated by
628 red drops, antigen density differences are represented by shades of blue circles. Fitting data
629 with generalized logistic curves yields two parameters, x_i and d, which characterize chemical
630 potential distribution of serum antibodies.

631

632 **Figure 2**. Fitting in two dimensions

633 Examples of parallel measurements of IgG and IgA binding to diagnostic celiac disease peptide
634 epitope are shown, with serum dilutions in three-fold (A) and two-fold (B) steps. Dot symbols
635 stand for measurement data, lines are fitted curves.

636

637 **Figure 3**. Comparative characterization of serum antibody binding

638 Using the values of the parameters obtained by curve fitting, calculated thermodynamic activity
639 coefficient distributions are comparable not only for serum samples (A) but also for distinct
640 antibody classes (B). Results shown in Figure 1 were used for the generation of normalized
641 comparisons. Bar charts (C) show mean d and x_i values, and 95% confidence intervals as
642 whiskers.

643

644 **Figure 4**. Conventional titration of serum.

645 Mid-point and end-point titers of IgA and IgG are calculated by logistic fitting of binding to
646 distinct antigen densities and are displayed as a function of antigen density.

647

648 **Figure 5**. Characterization of a monoclonal Ab for reference.

649 Binding data of monoclonal Ab 14D15 was fitted using the same algorithm as for serum
650 antibodies. Binding data and fitted curves (A), calculated distribution of activity coefficient (B)
651 and estimates of parameters x_i and d (C) are shown.

652

653 **Symbols and abbreviations**

654

655

a	relative thermodynamic activity
A	antibody capacity [FI]
Ab	antibody
[Ab]	antibody concentration [mol/L]
AbAg	antibody-antigen complex
[AbAg]	antibody-antigen complex concentration [mol/L]
Ag	antigen
[Ag]	antigen concentration [mol/L]
B	auxiliary parameter
BSA	Bovine Serum Albumin
c	molar concentration [mol/L]
C	auxiliary parameter
d	shape parameter that determines asymmetry
D	positive constant [L/mol]
ELISA	Enzyme-Linked Immunosorbent Assay
γ	thermodynamic activity coefficient
IgA	immunoglobulin A
IgG	immunoglobulin G
k	rate of exponential growth
K_D	equilibrium dissociation constant

m	auxiliary parameter
μ	chemical potential [J/mol]
μ^0	standard chemical potential [J/mol]
mAb	monoclonal antibody
PBS	Phosphate-Buffered Saline
R	ideal gas constant [~8.314 J/K*mol]
R(x)	Richards function
RFI	Relative Fluorescence Intensity
RIA	Radioimmunoassay
s	slope of lnR(x) at minus infinity
T	temperature [K]
x_i	value of x at inflection point
y_i	value of y at inflection point
z	serum dilution factor [1/dilution]

Figure 1. Simultaneous titration of antigen density and serum antibody

Steps of the technology, starting with microarray fabrication and measurement, through image analysis to curve fitting and visualization of results are shown. Serum dilution is indicated by red drops, antigen density differences are represented by shades of blue circles. Fitting data with generalized logistic curves yields two parameters, x_i and d, which characterize chemical potential distribution of serum antibodies.

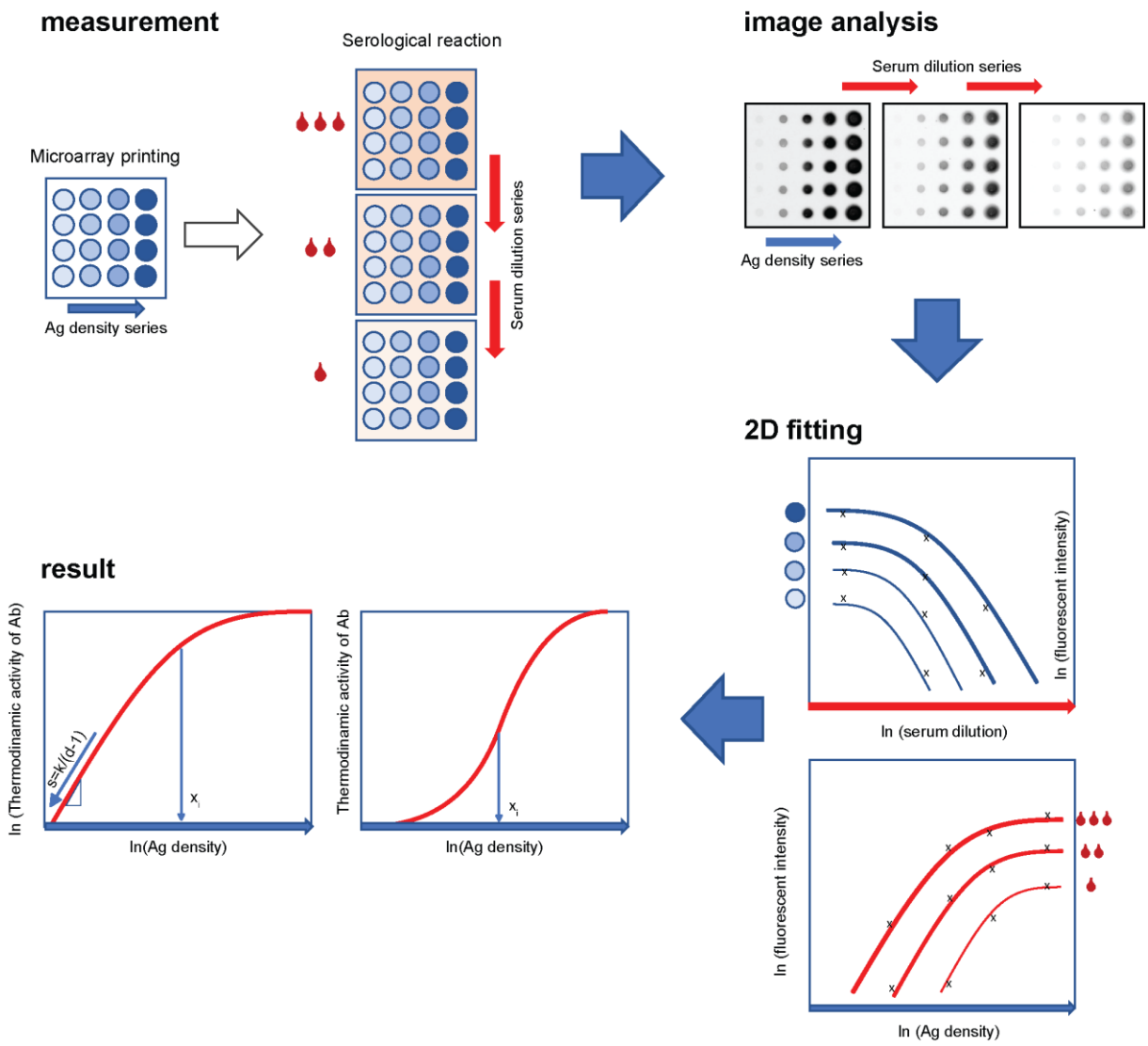

Figure 2. Fitting in two dimensions

Examples of parallel measurements of IgG and IgA binding to diagnostic celiac disease peptide epitope are shown, with serum dilutions in three-fold (A) and two-fold (B) steps. Dot symbols stand for measurement data, lines are fitted curves, numbers are sample identification numbers.

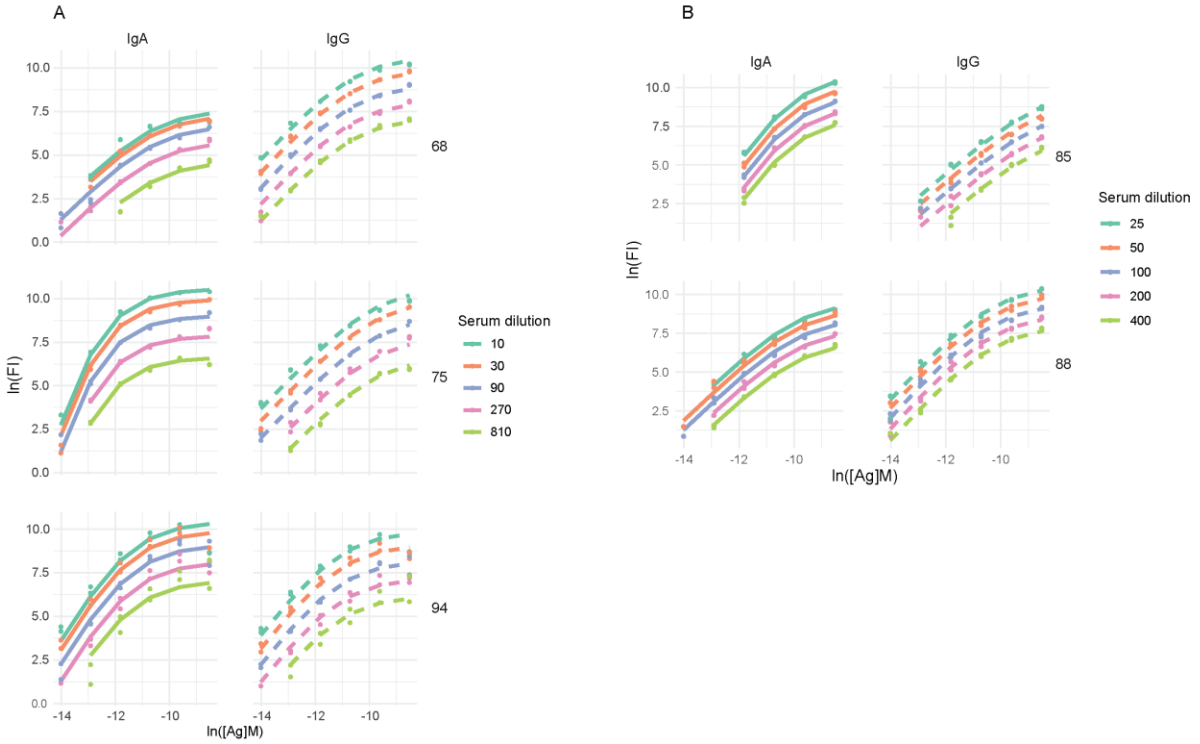

Figure 3. Comparative characterization of serum antibody binding

Using the values of the parameters obtained by curve fitting, calculated thermodynamic activity coefficient distributions are comparable not only for serum samples (A) but also for distinct antibody classes (B). Results from data shown in Figure 2 were used for the generation of normalized comparisons. Bar charts (C) show mean d and x_i values, and 95% confidence intervals as whiskers.

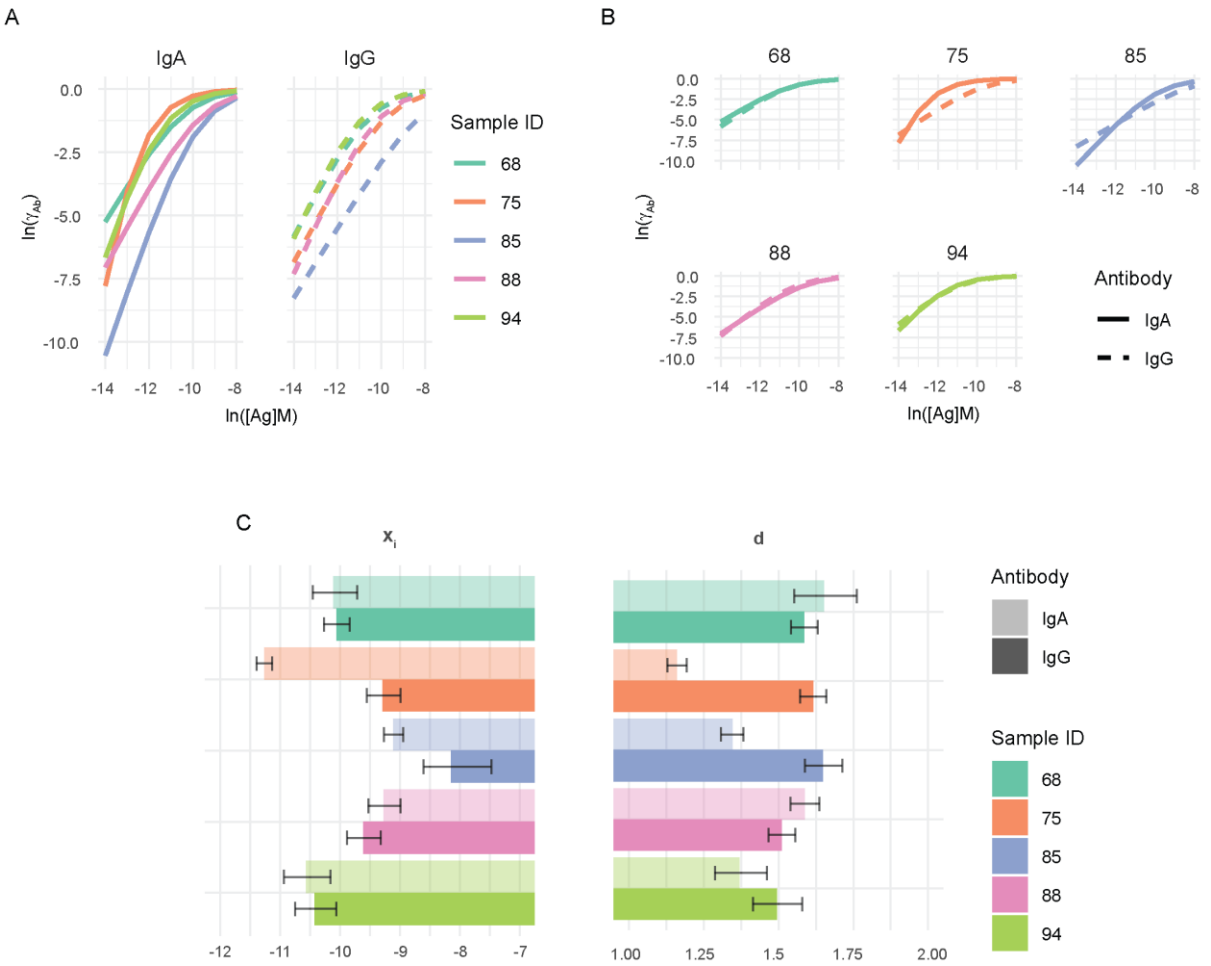

Figure 4. Conventional titration of serum.

Mid-point and end-point titers of IgA and IgG are calculated by logistic fitting of binding to distinct antigen densities and are displayed as a function of antigen density.

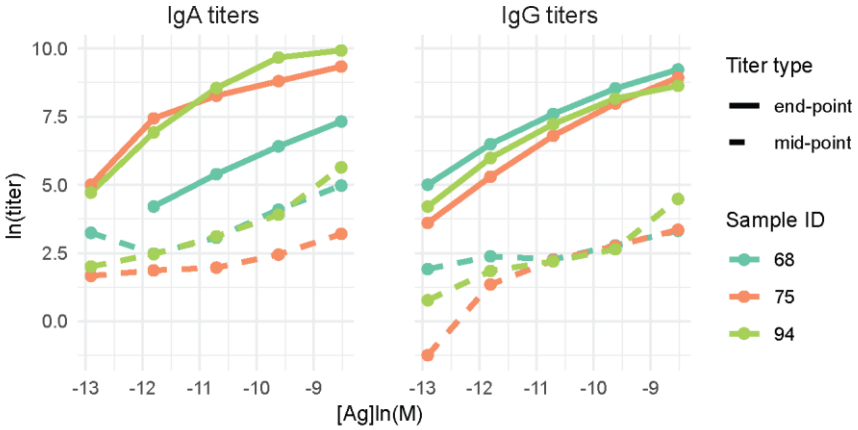

692

693 **Figure 5**. Characterization of a monoclonal Ab for reference.

694 Binding data of monoclonal Ab 14D15 was fitted using the same algorithm as for serum
695 antibodies. Binding data and fitted curves (A), calculated distribution of activity coefficient (B)
696 and estimates of parameters x_i and d (C) are shown.

697

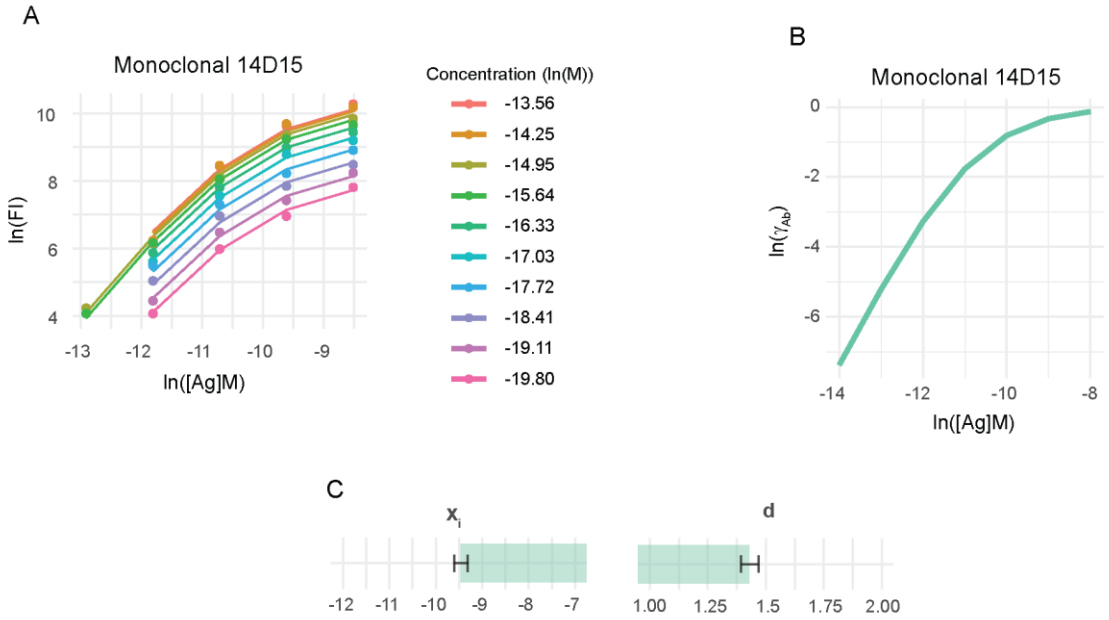

698
699